

Divergent Features of Mitochondrial Deficiencies in LGMD2A Associated With Novel Calpain-3 Mutations

Riyad El-Khoury, PhD, Sahar Traboulsi, BS, Tarek Hamad, BS, Maher Lamaa, MD, Raja Sawaya, MD, and Mamdouha Ahdab-Barmada, MD

Abstract

Limb girdle muscular dystrophy type 2A (LGMD2A) is an autosomal recessive disorder characterized by progressive muscle weakness and wasting. LGMD2A is caused by mutations in the calpain-3 gene (*CAPN3*) that encodes a Ca^{2+} -dependent cysteine protease predominantly expressed in the skeletal muscle. Underlying pathological mechanisms have not yet been fully elucidated. Mitochondrial abnormalities have been variably reported in human subjects with LGMD2A and were more systematically evaluated in *CAPN3*-knocked out mouse models. We have combined histochemical, immunohistochemical, molecular, biochemical, and ultrastructural analyses in our study in order to better outline mitochondrial features in 2 LGMD2A patients with novel *CAPN3*-associated mutations. Both patients underwent detailed clinical evaluations, followed by muscle biopsies from the quadriceps muscles. The diagnosis of LGMD2A in both patients was first suspected on the basis of a typical clinical localization of the muscle weakness, and confirmed by molecular investigations. Two novel homozygous mutations, c.2242C>G (p.Arg748Gly) and c.291C>A (p.Phe97Leu) were identified: c.2242C>G (p.Arg748Gly) mutation was associated with a significant mitochondrial mass depletion and myofibrillar disruption in the first patient, while c.291C>A (p.Phe97Leu) mutation was accompanied by reactive mitochondrial proliferation with ragged-red fibers in the second patient. Our results delineate *CAPN3* mutation-specific patterns of mitochondrial dysfunction and their ultrastructural characteristics in LGMD2A.

Key Words: Calpain-3, LGMD2A, Mitochondria, Novel mutations.

From the Neuromuscular Diagnostic Laboratory, Department of Pathology and Laboratory Medicine, American University of Beirut Medical Center, Beirut, Lebanon (RE-K, ST, TH, MA-B); Department of Pediatrics, Al Bahman Hospital, Beirut, Lebanon (ML); and Department of Neurology, American University of Beirut Medical Center, Beirut, Lebanon (RS).

Send correspondence to: Mamdouha Ahdab-Barmada, MD, Neuromuscular Diagnostic Laboratory, Department of Pathology and Laboratory Medicine, American University of Beirut Medical Center, Cairo Street, Beirut, Lebanon; E-mail: ma131@aub.edu.lb

This work was supported by the Lebanese Centre National de Recherche Scientifique (L-CNRS), Award number: 103508.

The authors have no duality or conflicts of interest to declare.

Supplementary Data can be found at academic.oup.com/jnen.

INTRODUCTION

Limb girdle muscular dystrophy type (LGMD2A) is an autosomal recessive disorder characterized by selective, slowly progressive weakness and wasting of the scapulothoracic and/or pelvifemoral girdle muscles (1). Impairment of ambulation often occurs 1 or 2 decades after diagnosis (2). The average onset of muscle weakness is in early adulthood with a wide spectrum that ranges from early childhood to the fifth decade of life (3, 4). LGMD2A is caused by loss-of-function mutations in the calpain-3 gene (*CAPN3*), which encodes a Ca^{2+} , Na^{+} -dependent cysteine protease (calpain-3) predominantly expressed in the skeletal muscle (5, 6). LGMD2A was reported as the most frequent autosomal recessive form of LGMD, averaging 30%–40% of all cases, with a significant geographical variation ranging from 9.2% in white US population to 80% in isolated communities (7, 8). Calpain-3 is mainly localized to the sarcomere of skeletal muscle fibers where it binds to the giant protein titin (9, 10). It is also found in the vicinity of the sarcoplasmic reticulum, in the triad region, where it interacts with the ryanodine receptor-1 (RYR-1) and calsequestrin (11). Thus, it appears that calpain-3 participates in many important physiological functions. Indeed, it has been shown that calpain-3 is essential to the control of sarcomere formation, maintenance, and remodeling (12–14). It is also essential for calcium uptake by the sarcoplasmic reticulum (15), cytoskeleton organization and remodeling (16, 17), and physical stress adaptation (18). In addition to its proteolytic activity, calpain-3 is characterized by a nonproteolytic structural function needed for various cellular processes, such as the regulation of Ca^{2+} release by the sarcoplasmic reticulum (11, 19). This duality may explain, at least in part, the wide spectrum of clinical symptoms and pathological features observed in LGMD2A. Moreover, calpain-3 can potentially have a large number of substrates and thus control multiple cellular processes, which makes it further difficult to discern pathological consequences and their underlying pathomechanisms. Isolated reports of mitochondrial dysfunction had been noted in human subjects, raising the need for more definite studies to confirm this possible factor in the evolving weakness observed with *CAPN3* mutations. Thus, further controlled studies conducted on calpain-3 knock out (C3KO) mice indicated that mitochondrial dysfunction may be a common finding associated with calpain-3 mutations (20, 21). It has been shown that mitochondrial biogenesis is impaired in regenerating cells from C3KO

mice when exposed to repeated cycles of cardiotoxin injections (22). Structural and functional abnormalities such as swollen mitochondria, decreased ATP production, and increased oxidative stress were also demonstrated in C3KO mice muscle, while mitochondrial biogenesis was shown to be increased (20). Another study by the same group using C3KO mice subjected to endurance exercise demonstrated a decrease in PGC1 α level, but its influence on mitochondrial mass and oxidative capacity were not indicated (21). Mitochondrial abnormalities were more difficult to ascertain in reported studies of LGMD2A patients even when detailed biochemical, histochemical, and electron microscopy studies were utilized (3, 23).

In this study, we have used histochemical, immunohistochemical, biochemical, and ultrastructural analysis in order to have a deeper insight into mitochondrial abnormalities repeatedly observed in patients with LGMD2A. Current investigations were performed on muscle biopsies obtained from 2 patients identified with novel mutations in the *CAPN3* gene. Our results confirmed the occurrence of mitochondrial deficiencies in both cases and more importantly delineated mutation-specific patterns of mitochondrial dysfunctions and their ultrastructural characteristics.

MATERIALS AND METHODS

Patients

Two young male patients from 2 nonrelated consanguineous families, 1 Lebanese and 1 Syrian, presented with recent onset of progressive muscle weakness with impaired gait and walking ability. Both patients underwent detailed clinical evaluations, followed by muscle biopsies taken from the quadriceps muscles. Research studies on human materials have been performed in accordance with the ethical standards laid down in the 1964 declaration of Helsinki and its later amendments. Oral and written consent was provided by the parents and patients to perform and report all needed tests for diagnostic evaluation.

Histochemical and Immunohistochemical Analysis

Freshly received muscle biopsies were oriented and processed as follows: Two cylinders were flash-frozen in liquid nitrogen-cooled 2-methylbutane (M32631, Sigma-Aldrich, Darmstadt, Germany) for histochemical and immunohistochemical evaluations of cross and longitudinal sections; 1 cylinder was fixed in 10% buffered formalin and processed for paraffin infiltration and sections; another tiny cylinder was immersed in glutaraldehyde/paraformaldehyde Karnovsky's solution to be processed for ultrastructural evaluation; residual tissue was bulk frozen in liquid nitrogen for biochemical and molecular studies if further needed.

Routine and other special stains were run on 6- μ m-thick sections (24, 25), including hematoxylin and eosin (H&E) and Masson's trichrome on paraffin sections; H&E, modified Gomori's trichrome, periodic acid Schiff (\pm diastase), Oil Red O, ATPase at pH 9.4 and 4.3, NADH, succinate dehydrogenase (SDH), cytochrome c oxidase (COX), and COX-SDH on

frozen sections. Immunohistochemistry (IHC) studies were also conducted on frozen sections and included IHC for ATP synthase (ab5432; 1:1000; Abcam, Numelab, Beirut, Lebanon), major histocompatibility complex (MHC) class I (ab52922; 1:750; Abcam, Numelab), C5b9 (ab55811; 1:250; Abcam, Numelab), and a panel of antibodies for dystrophic myopathies frequently observed in young patients. The panel included dystrophins N- and C-terminals and rod domain (NCL Dys-3,2,1; 1:20; Leica Biosystems, Paris, France), utrophin (NCL-DRP2; 1:10; Leica Biosystems), sarcoglycans (NCL A,B,D,G-SARC; 1:100; Leica Biosystems), dysferlin (NCL-Hamlet 1; 1:40; Leica Biosystems), caveolin-3 (610421; 1:300; BD Transduction Laboratories, Madrid, Spain), calpain-3 (Calp2C4, 1:100; Leica Biosystems), RYR-1 (ab59225; 1:50; Abcam, Numelab), SEPN1 (ab105943; 1:100; Abcam, Numelab), FKRP (ab65243; 1:50; Abcam, Numelab), dystroglycan A (ab64568; 1:50; Abcam, Numelab), dystroglycan B (NCL-b-DG; 1:50; Leica Biosystems), and laminins α 2 and 4 (NCL-merosin; 1:100; Leica Biosystems).

Ultrastructural Evaluation of Epon-Embedded Sections

Blocks of muscle tissue fixed in Karnovsky's solution (paraformaldehyde/glutaraldehyde) were stained with osmium and further processed and embedded into plastic (Epon). One-millimeter-thick sections from the Epon blocks were stained with toluidine blue and evaluated under light microscopy to select characteristic fields with diagnostic lesions. Selected ultrathin sections, cut from Epon-embedded blocks of tissue in cross and longitudinal orientation, were further stained with lead citrate and uranyl-acetate and evaluated with a transmission electron microscope. Photographs were examined to help clarify patterns of damage in both muscle biopsies.

Protein Extraction and Immunoblotting Analysis

Total protein extracts were obtained from a portion of muscle biopsies retrieved from patients and age-matched control individuals admitted for orthopedic care. Briefly, 50 mg of muscle tissue were disrupted mechanically in a PEBT3 buffer containing Tris-HCl at pH 6.8 (125 mM), SDS (5% v/v), EDTA (5 mM), glycerol (15% v/v), DTT (100 mM), and UREA (4 M). Homogenized tissues were then kept on ice for 10 minutes, heated at 95°C for 6 minutes and centrifuged at maximum speed for 10 minutes. Supernatant were collected and protein concentration was estimated using Bradford assay (26). Proteins (75 μ g) were separated on 4%–7% and 5%–11% denaturing polyacrylamide gels using the mini-PROTEAN Electrophoresis System from Bio-Rad (Marnes-La-Coquette, France) and blotted onto Amersham Hybond PVDF membrane (GE Healthcare). Cocktails of antibodies against either dystrophin (Dys2 C-terminus, 1:200; Leica Biosystems) and dysferlin (Hamlet, 1:300; Leica Biosystems), or calpain-3 (Calp2C4, 1:100; Leica Biosystems), caveolin-3 (ab2912, 1:400; Abcam, Numelab), α -sarcoglycan (ab189254, 1:1000; Abcam, Numelab), and β -dystroglycan (NCL-b-DG, 1:400; Leica Biosystems) were used to probe 4%–7% and 5%–11%

membranes, respectively. GAPDH (ab9484, 1:1500; Abcam, Numelab) was used as a loading control. Peroxidase conjugated antirabbit or antimouse secondary antibodies were used (ab6721 and ab6789, respectively, 1:1000; Abcam, Numelab). Signal was detected using a chemiluminescent-based method (Clarity Western ECL; Bio-Rad).

Biochemical Assessment of Mitochondrial Activities

Mitochondrial respiratory chain complexes activities (complexes I-V) and matrix associated enzymes (e.g. citrate synthase) were assessed in both patients using enzymatic-based spectrophotometric assays. Biochemical assessment was performed on homogenates prepared from portions of liquid nitrogen flash-frozen muscle biopsies. Spectrophotometric assays were conducted using a Cary 50 UV-visible spectrophotometer (Agilent Technologies; Varian, Inc., Les Ulis, France), as previously described (27).

Molecular Investigations

Genomic DNA was extracted from frozen muscle samples (20 mg) using the QIAamp DNA Mini Kit (51304; Qiagen, Hilden, Germany) following the manufacturer's instructions. *CAPN3* gene sequence was analyzed by next generation sequencing using a panel covering the 24 exons together with 50 bp of flanking intronic regions. Sequencing was based on Illumina sequencing technology, and all significant variants were validated by Sanger sequencing.

RESULTS

Clinical and Neurological Outcomes

Patient 1 was 9 years old at the time of his first evaluation for progressive weakness and increasing unsteadiness (Fig. 1A). Blood analysis showed elevated creatine kinase (CK) level of 3966 IU/L, progressively higher on monthly follow-ups and reaching 4977 IU/L, then 6750 IU/L. A first muscle biopsy was scheduled when CK level reached 7000 IU/L on the third month of follow-up. It was done at first in a small hospital with no provisions for special procedures. No frozen sections were evaluated, and a paraffin section was diagnosed as "Inflammatory myopathy consistent with polymyositis." The parents refused steroid therapy and took the child to consult a pediatric neurologist who noted pelvic girdle weakness more severely expressed than the usual proximal weakness, with absence of the typical Gower's maneuver sign. The child also had an impaired gait with walking difficulty. His "unstable gait" most likely reflected additional distal motor deficit. The neurologist noted that his older brother, 12 years old at the time of clinical evaluation of the 9-year-old current subject, presented similar but more advanced symptoms and a motor deficit that had also started at 9 years of age. Diagnostic work up had been declined for the older brother. A younger brother, then 4 years old, was clinically normal. Parents are maternal cousins, but no similar motor dysfunction had been reported among close relatives. A muscle biopsy was taken from the left vastus lateralis and was rapidly delivered

in the fresh state to our neuromuscular diagnostic lab for evaluation.

Patient 2 was 25 years old when he presented to the neurology clinic with a history of progressive weakness that had started in the left leg 7 years earlier (Fig. 1B). Clinical exam showed normal cranial nerves function, but diffuse generalized muscle atrophy sparing the trapezius muscles. Axial and proximal upper extremities weakness was characterized at 3+/5, with prominent winging. Deep tendon reflexes were absent. He had a waddling gait, marked weakness on standing up from squat position, mild paresthesia and numbness, and no clinical myotonia. His CK level was 1955 IU/L at the first evaluation and 1734 IU/L a month later at follow-up. All other laboratory evaluations, including ESR, ANA, and TSH levels, were within normal limits. Electromyogram (left deltoid, left extensor digitorum communis, right vastus medialis, and right tibialis anterior) showed severe generalized myopathy, increased polyphasia in the left deltoid and left extensor digitorum, motor units of low amplitude and short duration, and increased polyphasia in the right tibialis anterior with one myotonic discharge. Nerve conduction studies did not show any evidence of neuropathy. A muscle biopsy from the left quadriceps was taken, and findings suggested a dystrophic process as reported below. A repeat clinical evaluation was done 2 years later and included repeat electromyogram from the right biceps, the right vastus medialis, the right tibialis anterior and the right gastrocnemius, all indicating a severe progressive generalized myopathy affecting proximal and distal muscles in all extremities, consistent with evolving dystrophic process. His family history is pertinent as his parents were first degree cousins, but none of his 3 younger brothers showed clinical evidence of similarly evolving dystrophic process.

Muscle Biopsy: Histochemical and Immunohistochemical Features

Muscle biopsies of the left quadriceps (vastus lateralis) were performed on both patients as part of their diagnostic workup. Pathological assessment demonstrated dystrophic features in both patients, with variable mitochondrial characteristics. Patient 1 muscle biopsy showed marked variation in myofibers size and shape with scattered large dystrophic fibers, prominent endomysial fibrosis, and clusters of small regenerating myofibers (Fig. 2). Fiber splitting and myofibrillar disruption were frequent. Multifocal small areas of myofiber necrosis were highlighted by terminal complement complex (C5b9) deposits. Inflammatory infiltrates, mostly CD8⁺ T lymphocytes and CD68⁺ macrophages, with fewer CD20⁺ B lymphocytes, were scattered in endomysium near necrotic myofibers and also noted in perimysium surrounding small arterioles. Deposits of MHC I (MHC-1) coated regenerating myofibers. Immunohistochemical evaluation using a panel of antibodies to proteins involved in muscular dystrophies with childhood onset indicated normal protein expression over intact and regenerating myofibers away from necrotic foci, except for calpain-3 and RYR-1, which were markedly depleted. Histochemical assessment of mitochondrial respiratory chain enzymes activities, including NADH-TR, SDH, and COX, showed prominently depressed

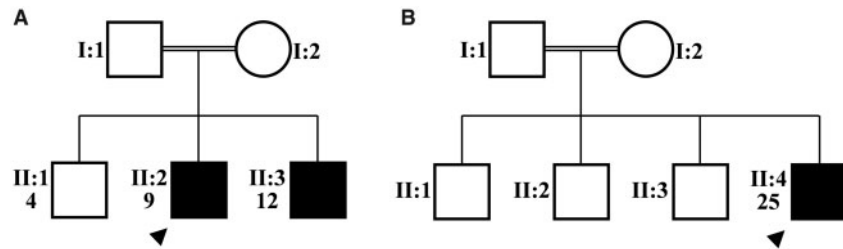


FIGURE 1. Pedigrees of 2 independent families based on LGMD2A features. **(A)** Lebanese family of 3 siblings from consanguineous parents (maternal cousins). **(B)** Syrian family of 4 siblings from consanguineous parents (first degree cousins). Proband is indicated by arrows. The Arabic numbers beneath the ID numbers represent the age of diagnosis. Filled and empty symbols indicate clinically affected (LGMD2A-positive) and nonaffected individuals, respectively. Double lines indicate consanguineous marriages (first degree cousins).

mitochondrial activity, with multifocal severe loss of activities imparting a “moth-eaten” appearance to most myofibers (Fig. 2). ATP synthase was also markedly depressed on immunohistochemical stain.

Patient 2 muscle biopsy showed widespread dystrophic features with marked variation in myofibers size and shape, numerous split myofibers, regenerating myofibers, many internalized nuclei and endomysial fibrosis (Fig. 3). Multifocal small areas of myofiber necrosis and clusters of small regenerating myofibers similar to those observed for patient 1 were also noted. The expression profile of proteins most commonly implicated in muscular dystrophies was normal as indicated by immunohistochemical stains except for calpain-3, which was completely absent. Some pathological features were, however, specific to patient 2. Pallor of central areas of many large dystrophic myofibers was prominent on histochemical stains of mitochondrial enzymes, while increased density and size of mitochondria was present within a peripheral subsarcolemmal rim of mildly increased mitochondrial activity within some of the myofibers. Loss of COX activity was total within a small number of type I myofibers. Scattered ragged-red fibers and many lobulated fibers were also noted (Fig. 3).

Transmission Electron Microscopy Studies

Ultrastructural study performed on the biopsy from patient 1 showed multifocal small areas of myofibrillar disruption, reminiscent of minicores, where mitochondria were absent and myofilaments disoriented, among streaming thickened Z bands. Clustered small and shrunken, often pyknotic mitochondria, some contained within phagocytic vacuoles, were also observed within many intermyofibrillar spaces and within subsarcolemmal “blebs,” both distended with background deposits of free, nonlysosomal bound accumulations of glycogen granules (Fig. 4A).

In patient 2, ultrastructural studies showed increased proliferation of subsarcolemmal and intermyofibrillar small, oval-shaped, or elongated mitochondria. Some of such mitochondria were occasionally pyknotic and collapsed, and some were partly degenerating into membranous profiles within autophagocytic vacuoles (Fig. 4B). In contrast to patient 1, no myofibrillar disorganization was noted.

Multiplex Immunoblotting Analysis

To further validate and expand immunohistochemical findings, we subsequently assessed by multiplex immunoblotting the steady state level of calpain-3 as well as several skeletal muscle proteins that are commonly involved in various muscular dystrophies. As shown in Figure 5, protein profiling indicated a complete absence of calpain-3 proteins in both patients when compared with the controls. Other assessed proteins, dystrophin, dysferlin, α -sarcoglycan, β -dystroglycan, and caveolin-3 (18 kDa) were normally expressed.

Biochemical Assessment of Mitochondrial Activities

Quantitative evaluation of mitochondrial respiratory chain complexes activities was assessed by enzymatic spectrophotometric assays on frozen muscle portions from both patients. A significant reduction in the activity of all respiratory chain complexes was noted in patient 1. Decreased activities were secondary to a substantial mitochondrial mass depletion as indicated by the activity of the reference enzyme citrate synthase (Table). All activities were within normal ranges for patient 2, and mitochondrial content remained within normal limits, as indicated by the activity of citrate synthase in this patient.

Molecular Analysis

Clinical and histological evaluations, and immunoblotting analysis, were indicative of an underlying dystrophic process suggestive of *calpain-3* deficiency and clinically involving limb girdle muscles in both patients. We attempted therefore to confirm a causative relation to calpainopathy by sequencing primarily the full-length of the *CAPN3* gene in both patients. Using high throughput sequencing, we identified 2 novel homozygous missense mutations c.2242C>G (p.Arg748Gly) and c.291C>A (p.Phe97Leu) in patients 1 and 2, respectively (Fig. 6). Both pathogenic homozygous variants were confirmed by Sanger sequencing. Moreover, the identification of an additional family member (elder sibling) of patient 1 harboring the pathogenic variant confirmed its segregation from heterozygous parents. No further molecular analysis could be conducted on the Syrian refugee family with

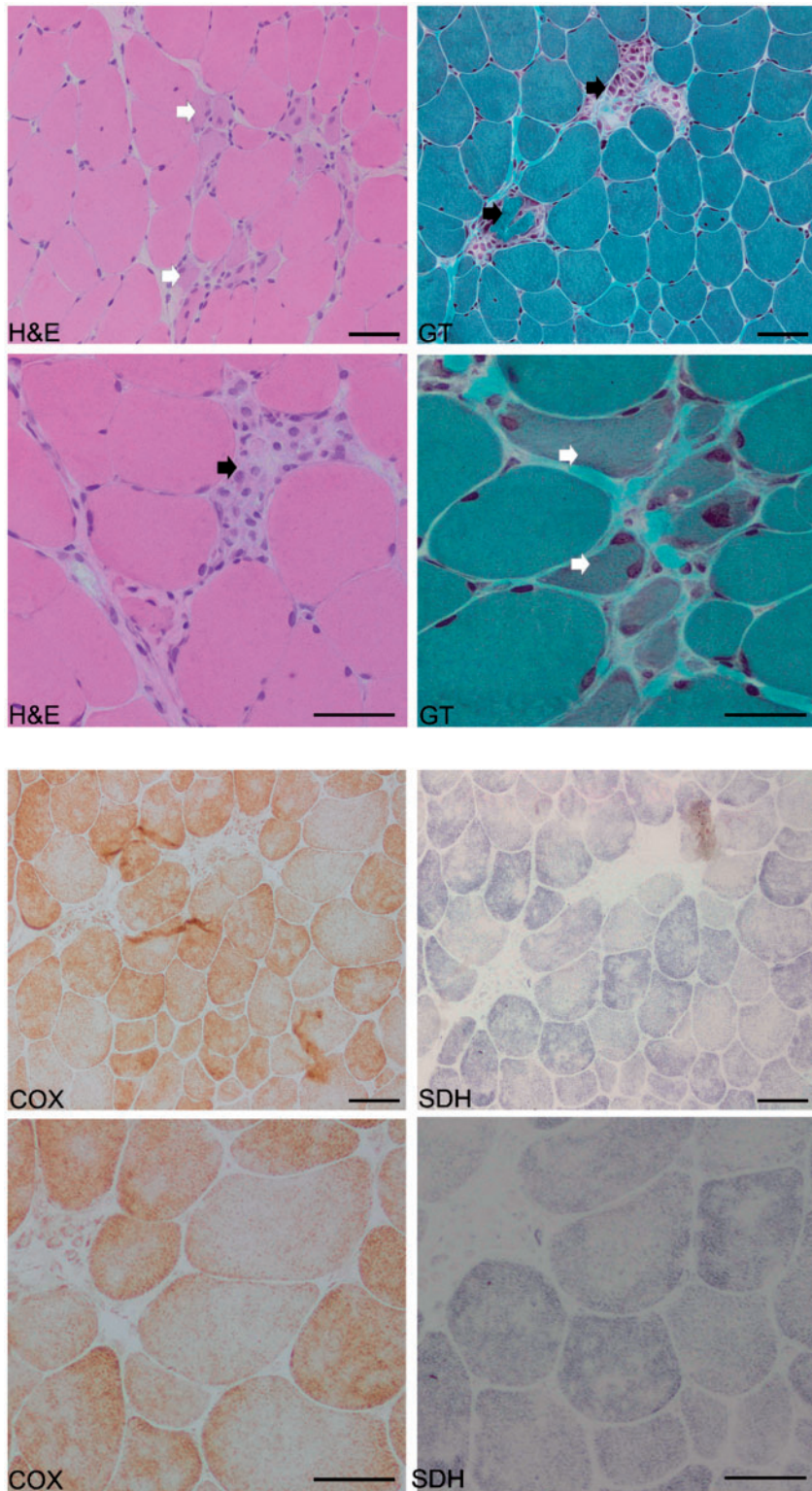


FIGURE 2. Muscle biopsy histology (patient 1). Hematoxylin and eosin (H&E) and modified Gomori’s trichrome (GT) stains show dystrophic features with fiber size variation, fiber splitting and endomysial fibrosis. Myofiber necrosis and myophagia (black arrows), and abnormally regenerating fibers (white arrows) are also observed. COX and SDH histoenzymatic reactions demonstrate a patchy pattern with “moth-eaten” appearance reflecting mitochondrial loss and myofibrillar network disruption. Upper and lower panels represent 100- and 200-fold magnification of sections, respectively. Scale bars: 50 μ m.

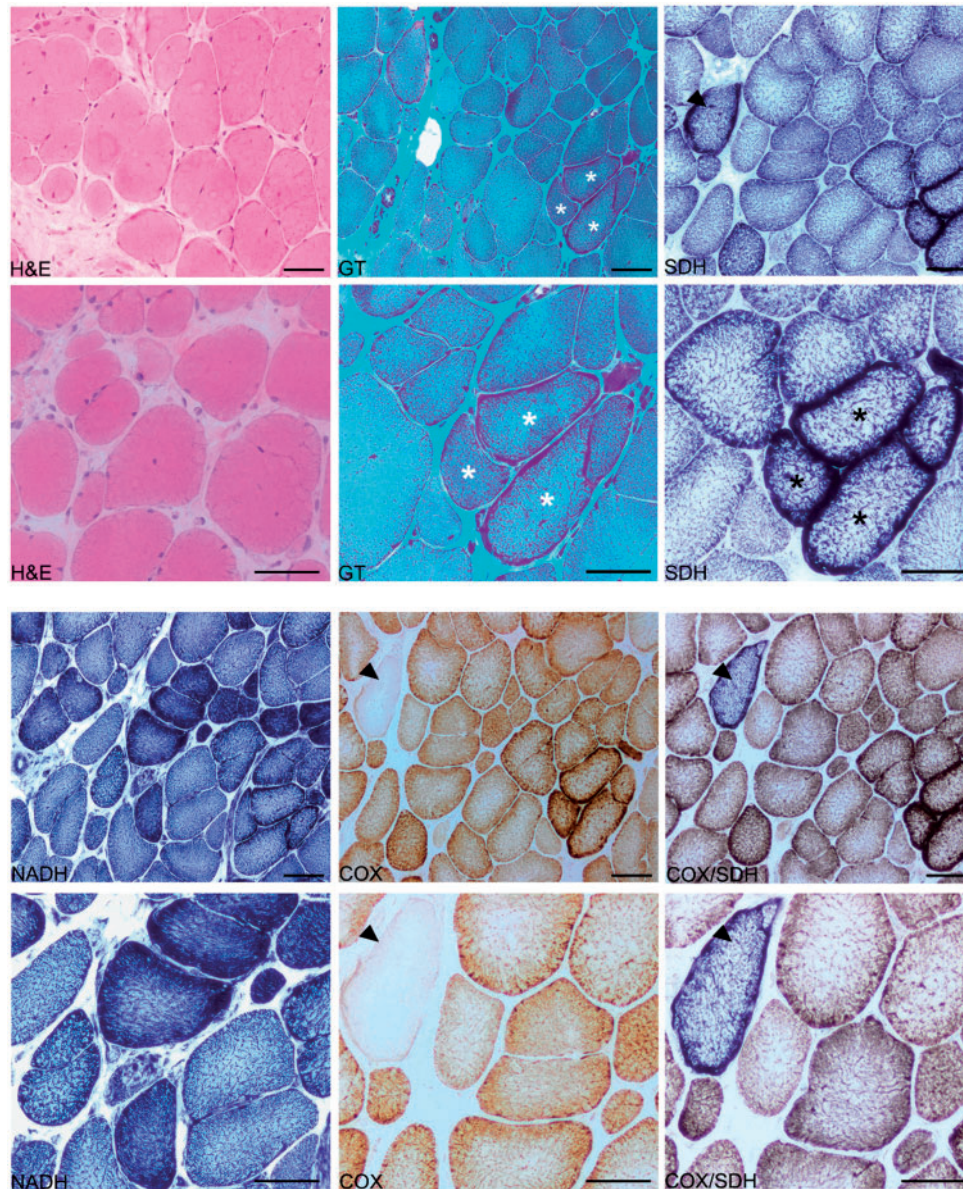


FIGURE 3. Muscle biopsy histology (patient 2). Hematoxylin and eosin (H&E) and modified Gomori's trichrome (GT) stains show endomysial fibrosis, fiber splitting, marked variation in myofibers size and shape, and clusters of ragged-red fibers (white asterisks). Pallor of central areas within many large dystrophic myofibers, subsarcolemmal accumulation of mitochondria (black asterisks), and occasional loss of COX activity within 2% of myofibers (black arrowhead) are noted on histochemical stains (COX, SDH and COX/SDH). Upper and lower panels represent 100- and 200-fold magnification of sections, respectively. Scale bars: 50 μ m.

which we have completely lost contact. Both variants had a strong pathogenicity prediction in tools such as CADD (<http://cadd.gs.washington.edu>), SIFT (<http://sift.jcvi.org>) and PolyPhen-2 (<http://genetics.bwh.harvard.edu>). Multiple sequence alignment analysis showed that the first mutation, c.2242C>G, resulted in the replacement of the highly conserved amino acid Arginine (p.Arg748) by a glycine in the PEF (Penta E-F hand) domain known to bind Ca^{2+} ions and to participate in protein dimerization. The second mutation resulted in the replacement of the less conserved phenylalanine

amino acid by a leucine residue in the N-terminal domain that is part of the catalytic core (Fig. 6).

DISCUSSION

Recessive mutations in *CAPN3* have been reported to cause LGMD2A, one of the most common forms of LGMD. A significant clinical and pathological variability is reported from different geographic areas of increased prevalence. Variability is also noted in the incidence, progression, clinical, and

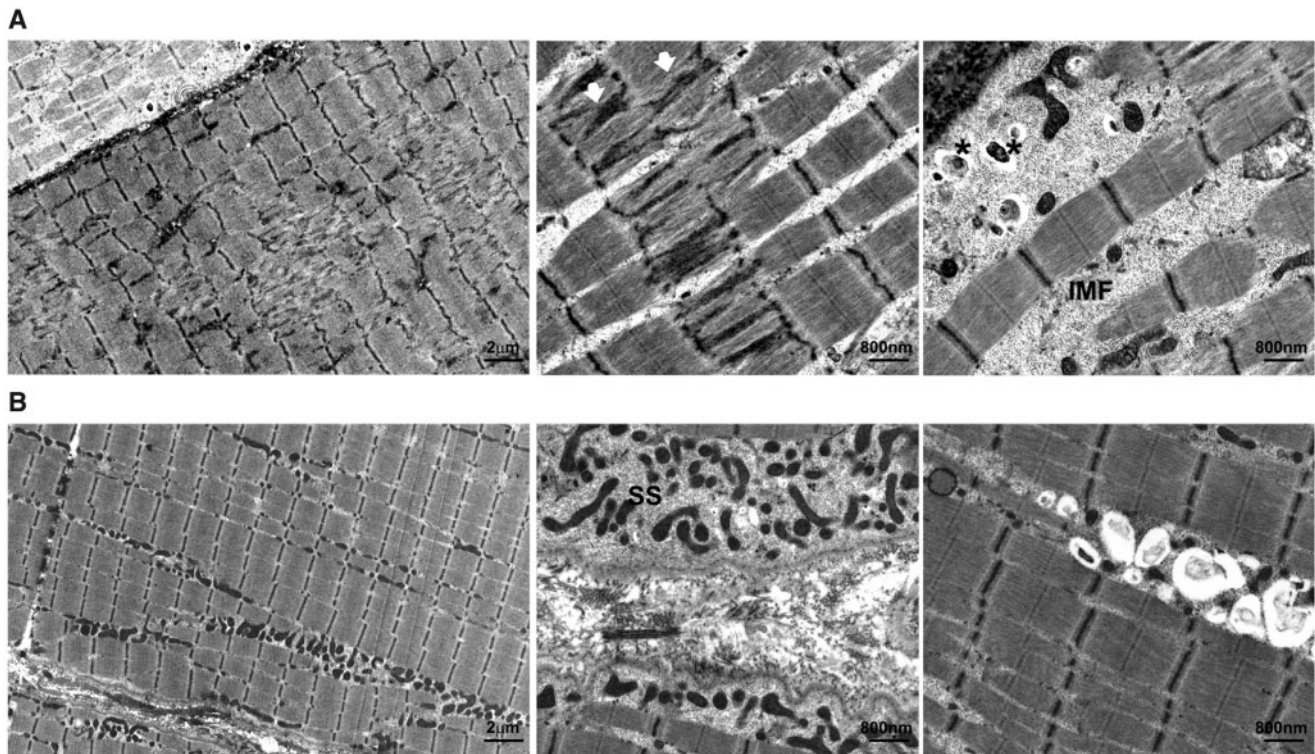


FIGURE 4. Ultrastructural analysis of probands' muscle biopsies. **(A)** In patient 1, left panel ($\times 2900$) and middle panel ($\times 9300$) sections show patchy myofibrillar disruption and Z bands streaming (white arrowhead). Abnormal often pyknotic mitochondria (right panel; $\times 9300$) (some contained within autophagic vacuoles) (asterisk) are noted in intermyofibrillar (IMF) and subsarcolemmal (SS) spaces. Glycogen granules density is increased in the distended IMF spaces and within SS blebs in both patients, more prominently in patient 1. **(B)** In patient 2, left panel ($\times 2900$) and higher middle panel ($\times 9300$) sections show focal SS and IMF proliferation of small and elongated mitochondria with indistinct internal profiles, some of which contained autophagic vacuoles (right panel; $\times 9300$). No myofibrillar disruptions were noted.

pathological characteristics observed among cases reported within the same family. According to the Leiden Muscular Dystrophy Mutation database, around 500 different pathogenic mutations, mostly missense mutations (50%–60%), have been identified to date.

To our knowledge, this is the first study to investigate the molecular, biochemical, structural, and ultrastructural bases of LGMD2A in Lebanon. We have identified 2 novel homozygous missense mutations in *CAPN3* in 2 nonrelated families. The first mutation, c.2242C>G (p.Arg748Gly), was identified in a 9-year-old child of a consanguineous (maternal cousins) Lebanese family while the second mutation c.291C>A (p.Phe97Leu) was identified in a member of another consanguineous (first degree cousins) Syrian family.

Clinical manifestations were at variance in both patients, possibly affected by the age of onset and rates of the disease progression, and also possibly related to the site and the type of mutation noted in the *CAPN3* gene in each patient. However, typical localization of the muscle weakness, involving most prominently axial muscles of the pelvic girdle and progressing to shoulder girdle, and to distal leg muscles, impairing gait and walking ability, was similar in both patients. Histological studies of muscle biopsies showed dystrophic patterns characterized mainly by increased variation in

myofibers size, focal clusters of small regenerating and atrophic myofibers, occasional degenerating and necrotic myofibers, increased endomysial fibrosis, and scanty inflammatory infiltrates. In addition, myofibers concomitantly expressing utrophin and dystrophin were frequently noted in both cases, possibly suggesting a delayed or disrupted maturation of affected myofibers.

Both patients showed absence of calpain-3 proteins by IHC and multiplex immunoblotting analysis. Yet, discrepancies were observed in the induced mitochondrial abnormalities illustrated in each one of the 2 patients. Mutation c.2242C>G was characterized by a significant “moth-eaten” appearance, with patchy myofibrillar disruption and a prominent decrease in mitochondrial oxidative enzymes activities on biochemical evaluation. Such depressed mitochondrial activities most probably resulted from (1) a significant reduction in the mitochondrial mass, reflected by a marked drop of the citrate synthase activity, and (2) an apparent lack of function of residual mitochondria as reflected by prominent pyknosis of the observed mitochondria in ultrastructural studies. Mutation c.291C>A induced pronounced mitochondrial proliferation in intermyofibrillar and subsarcolemmal spaces with features of “ragged-red” and “lobulated” myofibers on histochemical stains. Such mitochondrial proliferation is often observed in

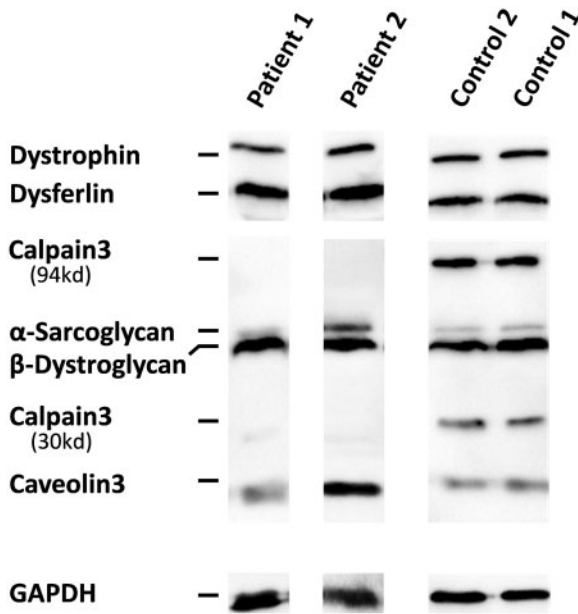


FIGURE 5. Multiplex immunoblotting analysis. Protein profiling by multiplex immunoblotting showed a complete absence of calpain-3 in both patients as compared to the controls. Dystrophin (423 kDa), dysferlin (200 kD), α -sarcoglycan (50 kDa), β -dystroglycan (43 kDa), and caveolin-3 (18 kDa) were normally expressed. GAPDH was used as a loading control.

muscle biopsies done to confirm a suspected mitochondrial dysfunction, and it is widely used as a diagnostic histological feature of potential mitochondrial dysfunction. Loss of COX activity within scattered myofibers was also noted. It is noteworthy that while histochemical stains and ultrastructural analysis highlighted disrupted mitochondrial distribution in the case of *c.291C>A* mutation, mitochondrial enzymatic activities remained within normal ranges on biochemistry studies (Table). Such results most likely reflect this reactive proliferation of mitochondria possibly triggered as an early defense mechanism in order to compensate for the ongoing disintegration, and loss, as observed in our ultrastructural studies (Fig. 4). Those findings highlight the importance of combining histochemical and biochemical studies when assessing mitochondrial activities, as subtle modifications maybe better delineated. No subsarcolemmal accumulation of mitochondria and no “lobulated fibers” were noted in the case of *c.2242C>G* mutation.

Ultrastructural studies allowed us to pinpoint an additional divergent phenotype between both mutations. Myofibrillar disruption and decreased mitochondrial population within patches of glycogen accumulation are noted in the case of *c.2242C>G* mutation (patient 1). Such myofibrillar disruption is reminiscent of the cores and minicores often observed with *SEPN1* and *RYR-1* mutations. Interestingly, *RYR-1* expression was significantly depleted in patient 1 and normal in patient 2 (Supplementary Data Fig. S1). This change may have been triggered by a specific loss of calpain-3 function in the control of *RYR-1* expression. Myofibrillar structure and

organization were fairly preserved in the case of *c.291C>A* mutation, and mitochondrial proliferating capacity was preserved, although mitochondrial survival appeared to be somewhat shortened, resulting in the appearance of pyknotic mitochondria within autophagic vacuoles.

LGMD2A is characterized by significant clinical and pathological variability between geographic backgrounds and even between siblings harboring the same mutation (28). The exact reasons leading to such disparities, and mainly those related to mitochondrial abnormalities, are still not clearly defined. Several studies over the last few years have attempted to shed light over such intriguing calpain-3 properties by delineating its intricate network of interactions and therefore unraveling some of its potential biological roles. It has been shown that calpain-3 plays an essential role in muscle regenerative capacity, mainly under physical stress conditions, through its catalytic activity. When sarcomeres extend, calpain-3 shift its location from the M-line region of Titin to its N2A region where it proteolyzes and activates several proteins implicated in modulating the signal transduction in response to external stress (18, 29, 30). Therefore, loss of calpain-3 activity may particularly explain the degenerative process observed in both our patients.

Several observations have also suggested that calpain-3 plays an important role in muscle maturation and differentiation (31). Our findings support such a role as myofibers in both patients showed a delayed maturation. Kramerova et al further demonstrated that, in *CAPN3* knocked out (*CAPN3-KO*) mouse model, Ca^{2+} /calmodulin-dependent protein kinase II (*Ca-CaMKII*) impairment resulted in an inefficient upregulation of *PGC-1 α* (21). The latter is a transcriptional coactivator that regulates broad programs of mitochondrial biology among which its respiratory capacity (32). Furthermore, a cardiotoxin-induced necrosis model has shown that AMP-activated protein kinase (AMPK) was significantly activated in *CAPN3-KO* regenerating muscle fibers (32). AMPK, the cellular sensor of ATP shortage, is known to stimulate slow fiber type gene expression and oxidative metabolism, while simultaneously inhibiting mTORC1 activity by direct phosphorylation. In skeletal muscles, mTORC1 enhances myofibrillar proteins synthesis and mitochondrial biogenesis, steering cellular growth and proliferation (33, 34). Accordingly, mTORC1 inhibition by AMPK was associated with failure to increase *PGC-1 α* transcripts and mitochondrial content in the regenerating *CAPN3-KO* muscles compared to WT (32).

In patients with LGMD2A, the outcomes of *CAPN3*-associated mutations on mitochondrial physiology and structure were highly variable among analyzed cases, and even dissimilar to those obtained in mice. Using enzymatic assays and Western blotting, Nilsson et al showed a preserved respiratory chain function in muscle biopsies of LGMD2A patients (35). Their data should, however, be taken cautiously as only a subset (5 out of 14) of their patients were analyzed enzymatically and only averages of those obtained values were reported rather than individual values, which might have averaged out values that would have been significantly different from those noted in the normal cases. In addition, no mitochondrial

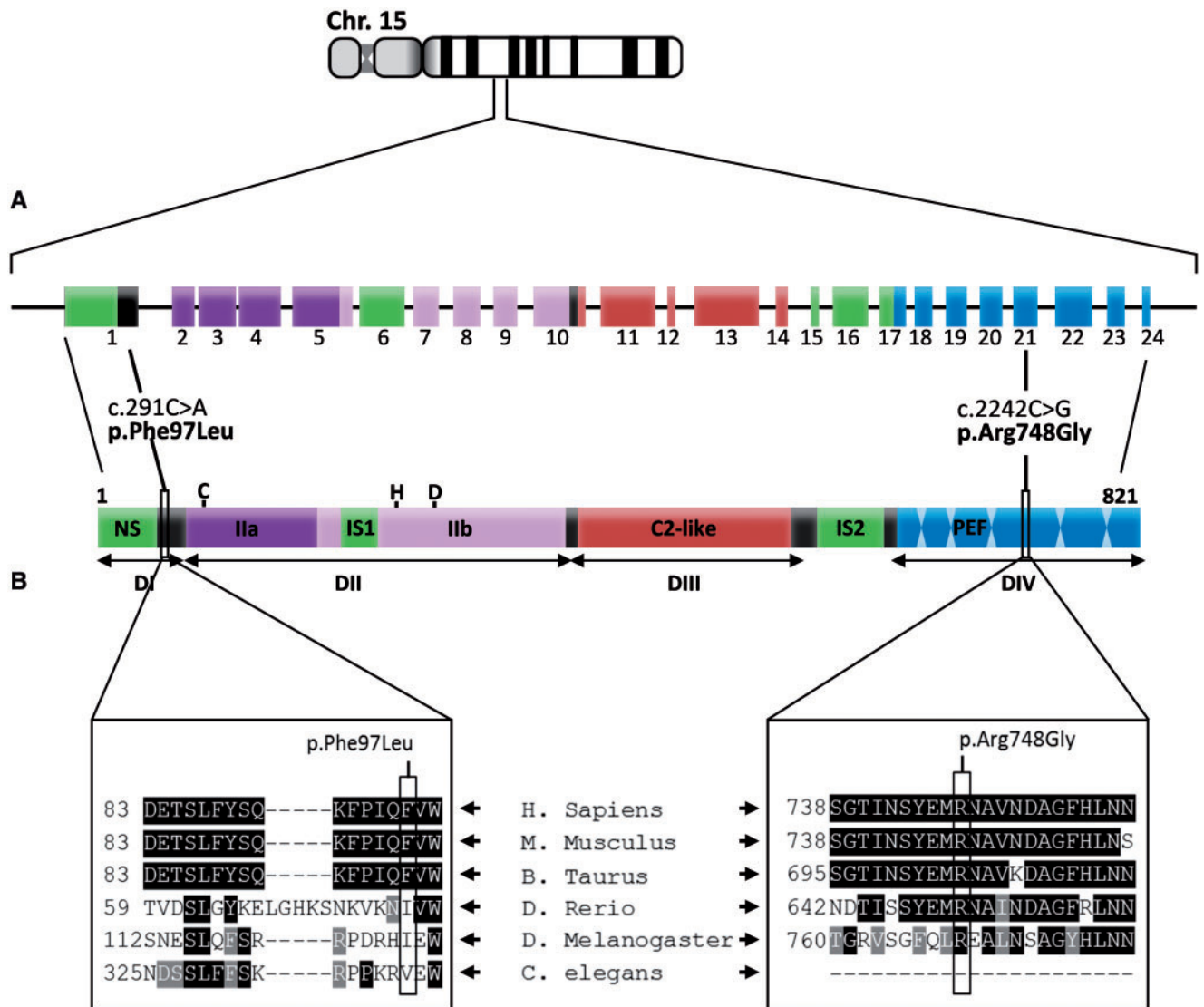


FIGURE 6. DNA sequencing of *CAPN3* gene and multiple sequence alignment. **(A)** Calpain-3 gene is localized on chromosome 15 (15q15.1). It comprises 24 exons and encodes an 821 amino acids multidomain protease. High throughput sequencing of the calpain-3 gene identified 2 novel homozygous mutations c.2242C>G (p.Arg748Gly) and c.291C>A (p.Phe97Leu) in patients 1 and 2, respectively. Mutation c.2242C>G is localized in exon 21 and involves an amino acid residue that is part of the PEF (Penta E-F hand) domain implicated in Ca²⁺ binding and protein dimerization. Mutation c.291C>A is localized in exon 1 and involves an amino acid residue that is part of the N-terminus (NS) domain that contains the nuclear localization signal. **(B)** Multiple sequence alignment of amino acids from different organisms indicated that p.Arg748 residue is evolutionary conserved among species whereas residue p.Phe97 was only conserved in mammals. The alignment was realized using the online software Clustal Omega (EMBL-EBI) with default parameters.

histochemical investigations were performed. Thus, possible correlations with putative focal loss or multifocal proliferation of mitochondria, as often noted in cases of mitochondrial dysfunction, were not outlined. Such correlations are important in cases where subtle modifications, for example, focal proliferation and/or degeneration, are suspected. In another study, by Pyle et al, respiratory chain dysfunction, with the occurrence of COX-negative fibers and mild reduction of complex IV activity, were noted in the skeletal muscle of an LGMD2A patient (36).

Our data indicate that some pathogenic variants, for example, c.2242C>G, mimic *CAPN3*-KO-associated phenotypes in their mitochondrial abnormalities, while others, for example, c.291C>A, induce divergent phenotypes. Thus, in addition to the pathogenic mechanisms described in *CAPN3*-KO mice, other factors and pathways may also be implicated in the onset of mitochondrial dysfunction associated with *CAPN3* mutations. It seems that the position of the mutation, the nature of the changed amino acid, and the induced consequences on structure, stability and various activities of the

TABLE. Biochemical Quantification of Mitochondrial Respiratory Chain Complexes Activities

	Activities (nmol/minute mg)		
	Patient1 (c.2242C>G)	Patient2 (c.291C>A)	Ref. Range (nmol/minute mg)
CI	5.10*	24.01	[10.42–47.30]
CII	2.44*	31.33	[18.73–47.70]
CIII	25.80*	124.99	[81.28–210.86]
CIV	17.98*	187.92	[82.01–237.59]
CV	20.09*	100.72	[62.21–130.72]
CII+III	8.50*	32.38	[16.21–33.24]
Citrate synthase	50.18*	142.25	[110.86–288.65]
LDH	4382	4979	[2084–7317]

Spectrophotometry-based assays were used in order to analyze enzymatic activities of NADH dehydrogenase (CI), succinate dehydrogenase (CII), coenzyme Q cytochrome c-oxidoreductase (CIII), cytochrome c oxidase (CIV) and ATPase (CV). Citrate synthase activity was used as a control for mitochondrial mass, while lactate dehydrogenase (LDH) was used as a cytosolic reference. Normalized activities, expressed in terms of the citrate synthase level for each individual complex were within normal ranges in both cases. Values represent enzymatic activities and are expressed in nanomoles of substrate transformed per minute per milligrams of proteins (nmol/minute mg).

*Indicates activities that do not fall within our normal reference values.

calpain-3 protein deeply impact the progression of the disorder and dictate disease outcomes. Some *CAPN3* delineated mutations were shown to accelerate the autolytic activity of calpain-3, leading to its loss even before it could accomplish its various activities (37, 38), while other mutations were shown to affect calpain-3 conformation in a way that altered substrate recognition and/or posttranslational regulatory sites (19, 39). Further mutations may affect solely the proteolytic activity of calpain-3 without modifying its nonproteolytic function (11).

The first missense mutation c.2242C>G that we have identified is localized in exon 21 and involves an evolutionary conserved amino acid, p.Arg748, which is part of the calpain-3 PEF domain known to bind Ca²⁺ ions and to participate in protein dimerization as well as substrate recognition. The second missense mutation c.291C>A is localized in exon 1 and involves the amino acid p.Phe97 of the N-terminal domain that is part of the catalytic core. Contrarily to Arg748 amino acid, Phe97 is mainly conserved among mammalian species while divergent in others. In both of our cases we observed a complete loss of calpain-3 proteins whether by immunoblotting or by IHC. Identifying the mechanism leading to mitochondrial abnormalities at the origin of possibly divergent clinical and pathological outcomes remains putative. Novel insights are needed for further understanding of the multiple pathogenetic mechanisms and their observed variabilities.

Our data suggest that *CAPN3*-associated mutations lead to possibly defective activation and rapid alteration of various signaling pathways, leading ultimately to potential mutation-specific mitochondrial deficiencies. The existence of genetic modifiers may also play a role in the variability of clinical outcomes, even within members of the same family. Secondary deficiencies might contribute significantly to the development of specific clinical phenotypes. Such findings should raise

awareness regarding novel targeted therapies. Clarification of functional pathophysiological processes implicated in the onset and progression of muscular dystrophies may help improve clinical applications of existing therapies independently of the primary cause of the disease.

REFERENCES

1. Fanin M, Angelini C. Protein and genetic diagnosis of limb girdle muscular dystrophy type 2A: The yield and the pitfalls. *Muscle Nerve* 2015;52:163–73
2. Bushby KM. The muscular dystrophies. *Baillieres Clin Neurol* 1994;3:407–30
3. Chae J, Minami N, Jin Y, et al. Calpain 3 gene mutations: Genetic and clinico-pathologic findings in limb-girdle muscular dystrophy. *Neuromuscul Disord* 2001;11:54755
4. Straub V, Bertoli M. Where do we stand in trial readiness for autosomal recessive limb girdle muscular dystrophies? *Neuromuscul Disord* 2016;26:111–25
5. Goll DE, Thompson VF, Li H, et al. The calpain system. *Physiol Rev* 2003;83:731–801
6. Ono Y, Ojima K, Torii F, et al. Skeletal muscle-specific calpain is an intracellular Na⁺-dependent protease. *J Biol Chem* 2010;285:22986–98
7. Urtasun M, Sáenz A, Roudaut C, et al. Limb-girdle muscular dystrophy in Guipúzcoa (Basque Country, Spain). *Brain J Neurol* 1998;121:1735–47
8. Chou FL, Angelini C, Daentl D, et al. Calpain III mutation analysis of a heterogeneous limb-girdle muscular dystrophy population. *Neurology* 1999;52:1015–20
9. Sorimachi H, Kinbara K, Kimura S, et al. Muscle-specific calpain, p94, responsible for limb girdle muscular dystrophy type 2A, associates with connectin through IS2, a p94-specific sequence. *J Biol Chem* 1995;270:31158–62
10. Keira Y, Noguchi S, Minami N, et al. Localization of calpain 3 in human skeletal muscle and its alteration in limb-girdle muscular dystrophy 2A muscle. *J Biochem (Tokyo)* 2003;133:659–64
11. Ojima K, Ono Y, Ottenheim C, et al. Non-proteolytic functions of calpain-3 in sarcoplasmic reticulum in skeletal muscles. *J Mol Biol* 2011;407:439–49
12. Kramerova I, Kudryashova E, Venkatraman G, et al. Calpain 3 participates in sarcomere remodeling by acting upstream of the ubiquitin-proteasome pathway. *Hum Mol Genet* 2005;14:2125–34
13. Beckmann JS, Spencer M. Calpain 3, the “gatekeeper” of proper sarcomere assembly, turnover and maintenance. *Neuromuscul Disord* 2008;18:913–21
14. Baghdiguian S, Martin M, Richard I, et al. Calpain 3 deficiency is associated with myonuclear apoptosis and profound perturbation of the IκappaB alpha/NF-kappaB pathway in limb-girdle muscular dystrophy type 2A. *Nat Med* 1999;5:503–11
15. Michel LYM, Hoenderop JGJ, Bindels RJM. Calpain-3-mediated regulation of the Na⁺-Ca²⁺ exchanger isoform 3. *Pflugers Arch* 2016;468:243–55
16. Guyon JR, Kudryashova E, Potts A, et al. Calpain 3 cleaves filamin C and regulates its ability to interact with gamma- and delta-sarcoglycans. *Muscle Nerve* 2003;28:472–83
17. Kramerova I, Beckmann JS, Spencer MJ. Molecular and cellular basis of calpainopathy (limb girdle muscular dystrophy type 2A). *Biochim Biophys Acta* 2007;1772:128–44
18. Ojima K, Kawabata Y, Nakao H, et al. Dynamic distribution of muscle-specific calpain in mice has a key role in physical-stress adaptation and is impaired in muscular dystrophy. *J Clin Invest* 2010;120:2672–83
19. Ono Y, Ojima K, Shinkai-Ouchi F, et al. An eccentric calpain, CAPN3/p94/calpain-3. *Biochimie* 2016;122:169–87
20. Kramerova I, Kudryashova E, Wu B, et al. Mitochondrial abnormalities, energy deficit and oxidative stress are features of calpain 3 deficiency in skeletal muscle. *Hum Mol Genet* 2009;18:3194–205
21. Kramerova I, Ermolova N, Eskin A, et al. Failure to up-regulate transcription of genes necessary for muscle adaptation underlies limb girdle muscular dystrophy 2A (calpainopathy). *Hum Mol Genet* 2016;25:2194–207

22. Yalvac ME, Amornvit J, Braganza C, et al. Impaired regeneration in calpain-3 null muscle is associated with perturbations in mTORC1 signaling and defective mitochondrial biogenesis. *Skeletal Muscle* 2017;7:27
23. Kawai H, Akaike M, Kunishige M, et al. Clinical, pathological, and genetic features of limb-girdle muscular dystrophy type 2A with new calpain 3 gene mutations in seven patients from three Japanese families. *Muscle Nerve* 1998;21:1493–501
24. Loughlin M. *Muscle Biopsy: A Laboratory Investigation*. Oxford: Butterworth-Heinemann; 1993.
25. Dubowitz V, Sewry CA, Oldfors A, Lane RJM. *Muscle Biopsy: A Practical Approach, 4th Edition*. Oxford: Saunders, 2013. Available from: <http://www.clinicalkey.com/dura/browse/bookChapter/3-s2.0-C2009063539X> [cited April 26, 2018]
26. Bradford MM. A rapid and sensitive method for the quantitation of microgram quantities of protein utilizing the principle of protein-dye binding. *Anal Biochem* 1976;72:248–54
27. Rustin P, Chretien D, Bourgeron T, et al. Biochemical and molecular investigations in respiratory chain deficiencies. *Clin Chim Acta Int Acta* 1994;228:35–51
28. Guglieri M, Magri F, D'Angelo MG, et al. Clinical, molecular, and protein correlations in a large sample of genetically diagnosed Italian limb girdle muscular dystrophy patients. *Hum Mutat* 2008;29:258–66
29. Ojima K, Ono Y, Doi N, et al. Myogenic stage, sarcomere length, and protease activity modulate localization of muscle-specific calpain. *J Biol Chem* 2007;282:14493–504
30. Hayashi C, Ono Y, Doi N, et al. Multiple molecular interactions implicate the connectin/titin N2A region as a modulating scaffold for p94/calpain 3 activity in skeletal muscle. *J Biol Chem* 2008;283:14801–14
31. Spencer MJ, Guyon JR, Sorimachi H, et al. Stable expression of calpain 3 from a muscle transgene in vivo: Immature muscle in transgenic mice suggests a role for calpain 3 in muscle maturation. *Proc Natl Acad Sci USA* 2002;99:8874–9
32. Rowe GC, Patten IS, Zsengeller ZK, et al. Disconnecting mitochondrial content from respiratory chain capacity in PGC-1-deficient skeletal muscle. *Cell Rep* 2013;3:1449–56
33. Atherton PJ, Babraj J, Smith K, et al. Selective activation of AMPK-PGC-1 α or PKB-TSC2-mTOR signaling can explain specific adaptive responses to endurance or resistance training-like electrical muscle stimulation. *FASEB J* 2005;19:786–8
34. Baar K. Training for endurance and strength: Lessons from cell signaling. *Med Sci Sports Exerc* 2006;38:1939–44
35. Nilsson MI, Macneil LG, Kitaoka Y, et al. Redox state and mitochondrial respiratory chain function in skeletal muscle of LGMD2A patients. *PLoS One* 2014;9:e102549
36. Pyle A, Nightingale HJ, Griffin H, et al. Respiratory chain deficiency in nonmitochondrial disease. *Neurol Genet* 2015;1:e6
37. Ono Y, Shimada H, Sorimachi H, et al. Functional defects of a muscle-specific calpain, p94, caused by mutations associated with limb-girdle muscular dystrophy type 2A. *J Biol Chem* 1998;273:17073–8
38. Diaz BG, Moldoveanu T, Kuiper MJ, et al. Insertion sequence 1 of muscle-specific calpain, p94, acts as an internal propeptide. *J Biol Chem* 2004;279:27656–66
39. Keira Y, Noguchi S, Kurokawa R, et al. Characterization of lobulated fibers in limb girdle muscular dystrophy type 2A by gene expression profiling. *Neurosci Res* 2007;57:513–21